J. Fluid Mech. (2008), *vol.* 606, *pp.* 225–237.
doi:10.1017/S0022112008001675 Printed in the United Kingdom

Statistical structure of momentum sources and sinks in the outer region of a turbulent boundary layer

B. GANAPATHISUBRAMANI

Department of Aeronautics, Imperial College London,
Prince Consort Road, South Kensington, London, SW7 2AZ, UK
g.bharath@imperial.ac.uk

(Received 21 January 2008 and in revised form 27 March 2008)

The spatial structure of momentum sources and sinks ($T > 0$ and $T < 0$; where T is the streamwise component of the Lamb vector) is examined in a turbulent boundary layer by using dual-plane particle image velocimetry data obtained in streamwise–spanwise planes at two wall-normal locations ($x_2/\delta = 0.1$ and 0.5, where x_2 is the wall-normal location and δ is the boundary layer thickness). Two-point correlations of T indicate that the size of source motions remains relatively constant while the size of sink motions increases with increasing wall-normal distance. The relative strength of sink motions also increases away from the wall. The velocity field in the vicinity of source/sink motions was explored by computing cross-correlations of T with the velocity components. Source-like motions are correlated with elongated low-momentum zones that possess regions of upwash embedded within them and appear to be the strongest in areas where these low-momentum zones meander in the spanwise direction. Momentum sinks appear to be located within low-speed regions that are within larger high-momentum zones. The velocity fluctuations undergo rapid transitions between quadrants in the vicinity of sinks (i.e. both streamwise and wall-normal velocity fluctuations change sign). The length scales, over which the fluctuations change sign, are much larger at $x_2/\delta = 0.5$ than at $x_2/\delta = 0.1$.

1. Introduction

The flow structure of Reynolds-shear-stress-producing events in turbulent boundary layers is well documented. Some of the features that are relevant to Reynolds stress production and transport include hairpin/cane vortices (see Theodorsen 1952 among others), sweeps and ejections (Wallace, Eckelmann & Brodkey 1972; Willmarth & Lu 1972; Blackwelder & Kaplan 1976 and others), superbursts (Na, Hanratty & Liu 2001), hairpin packets (Adrian, Meinhart & Tomkins 2000), and large-scale and very large-scale motions (LSM and VLSM, see Kim & Adrian 1999).

While most research focuses on Reynolds shear stress events, inspection of the mean momentum equation indicates that the gradient of Reynolds shear stress is of primary importance to the rate of change of momentum. For a boundary layer, the mean momentum equation shows that the wall-normal gradient of mean Reynolds shear stress ($\overline{T}$), which is the time-averaged effect of turbulent advection, is a force-like quantity that acts as a momentum source/sink:

$$U_1\frac{\partial U_1}{\partial x_1} + U_2\frac{\partial U_1}{\partial x_2} = \nu\frac{\partial^2 U_1}{\partial {x_2}^2} + \overline{T} \tag{1.1}$$

where

$$T = \frac{\partial(-u_1 u_2)}{\partial x_2}. \tag{1.2}$$

In this study, the streamwise, wall-normal and spanwise directions are along the x_1-, x_2- and x_3-axes respectively. The mean and fluctuating velocity components along those three directions are represented by (U_1, U_2, U_3) and (u_1, u_2, u_3), respectively. The kinematic viscosity is ν and $u_1 u_2$ is the instantaneous Reynolds shear stress (also known as the shear product). The overline indicates time-averaged quantities.

Examination of wall-normal variation of mean Reynolds shear stress in wall-bounded flows reveals a single peak position (x_{2p}). At this peak, the gradient of mean Reynolds shear stress is zero. Therefore, the term $\overline{T}$ acts as a momentum source for $x_2 < x_{2p}$ (where $\partial[-\overline{u_1 u_2}]/\partial x_2 > 0$) and as a sink for $x_2 > x_{2p}$ (where $\partial[-\overline{u_1 u_2}]/\partial x_2 < 0$). Wei *et al.* (2005) explored the mean momentum balance based on experimental and direct numerical simulation (DNS) data and observed the existence of a four-layer structure for wall-bounded flows where the wall-normal extent of the layers depends on the relative magnitude of $\overline{T}$ compared to the viscous term. Therefore, there is great interest in exploring the structure of T to understand the motions that contribute to the mean–momentum balance.

The wall-normal gradient of Reynolds shear stress in an incompressible flow can be expanded as follows (see Hinze 1975 among others):

$$\overline{T} = \overline{[u \times \omega]_1} - \frac{1}{2}\frac{\partial}{\partial x_1}\left(\overline{u_1^2} - \overline{u_2^2} - \overline{u_3^2}\right) \tag{1.3}$$

where

$$[u \times \omega]_1 = u_2\omega_3 - u_3\omega_2 \tag{1.4}$$

where $[u \times \omega]_1$ is the streamwise component of the Lamb vector and (ω_1, ω_2, ω_3) are the fluctuating components of vorticity along the (x_1, x_2, x_3)-directions. Klewicki (1989) explored the wall-normal gradient of Reynolds shear stress and concluded that it is dominated by the velocity–vorticity correlation. He documented that other terms in the above equation (i.e. the streamwise gradient of turbulent intensities) are three orders of magnitude smaller than the velocity–vorticity term. This suggests that the velocity–vorticity interactions play a dominant role in producing motions that are capable of acting as either momentum sources or sinks. Therefore, the characteristics of source/sink motion can be explored by examining the structure of $[u \times \omega]_1$.

A few researchers have investigated the motions that contribute to the velocity–vorticity correlation, including the aforementioned studies by Klewicki (1989). Subsequent results from Rovelstadt (1991) (numerical) and Ong (1992) (experimental) were consistent with the results obtained by Klewicki (1989). Rajagopalan & Antonia (1993) studied the structure of the velocity field associated with the spanwise vorticity field and reported cross-correlations of $u_2\omega_3$ and $u_1\omega_3$. They concluded that the velocity signature is consistent with the presence of internal shear layers, inclined to the wall. Klewicki, Murray & Falco (1994) investigated the $u_2\omega_3$ term in the near-wall region and concluded that the existence of positive spanwise vorticity for $x_2^+ > 12$ is consistent with the presence of a ring-like eddy (the superscript $+$ is used to denote quantities that are normalized with skin friction velocity u_τ and ν). Klewicki & Hirsch (2004) performed combined hot-wire/flow visualization measurements near the wall and found that $u_2\omega_3$ local to near-wall shear layers tends to attenuate the near-wall Reynolds stress gradient.

Guala, Hommema & Adrian (2006) computed the wall-normal derivative of the u_1u_2 co-spectra in a pipe flow across a range of wall-normal locations and concluded that very-large scale motions (VLSMs) make a significant contribution to the net Reynolds shear force. Priyadarshana *et al.* (2007) compared the velocity–vorticity correlations over a wide range of Reynolds numbers and found that the interaction between velocity and vorticity depends on the Reynolds number and wall roughness. They proposed a model where approximately uniform momentum zones (consistent with VLSMs) are intermittently segregated by narrow fissures of highly vortical flow. However, they acknowledged that their model only provides a description of how the different scales of motion in the velocity and vorticity fields might interact. The specific interactions that generate positive or negative Reynolds shear stress force and the structure of momentum source/sink-like motions are not clear.

In the current study, the spatial structure of the streamwise component of the Lamb vector ($[u \times \omega]_1$) is explored using dual-plane particle image velocimetry (PIV) data to classify the motions that act as momentum sources and sinks.

2. Experiments

The experiments that form the basis for this work were carried out by Ganapathisubramani (2004) at the University of Minnesota in a suction-type wind tunnel. Measurements were obtained 3.3 m downstream of a trip wire in a zero-pressure-gradient turbulent boundary layer with a free-stream velocity (U_∞) of 5.9 $\mathrm{m\,s^{-1}}$. The relevant parameters in the region of measurements were as follows: skin friction velocity $u_\tau = 0.24\ \mathrm{m\,s^{-1}}$, Kármán number $\delta^+ = \delta u_\tau/\nu = 1100$ (where δ is the boundary layer thickness) and Reynolds number based on the momentum thickness $Re_\theta = 2800$.

Simultaneous dual-plane PIV experiments, which utilized three cameras to measure velocity components in two differentially separated planes (separated by 1.3 mm, i.e. 21 wall units), were performed in streamwise–spanwise planes. Stereoscopic data were obtained in one plane with two cameras, and standard PIV data were obtained in the other with a single camera. The acquired datasets were used in tandem with the continuity equation to calculate the complete velocity gradient tensor. Further details of the experimental setup, uncertainty analysis and validation can be found in Ganapathisubramani (2004), Ganapathisubramani *et al.* (2005*b*) and Ganapathisubramani, Longmire & Marusic (2006).

The measurement domain size is $1.1\delta \times 1.1\delta$ and 1000 statistically independent realizations were obtained at two wall-normal locations, ${x_2}^+ = 110$ ($x_2/\delta \approx 0.1$) and ${x_2}^+ = 575$ ($x_2/\delta \approx 0.5$). The availability of complete instantaneous velocity and velocity gradient tensor information enabled the computation of the instantaneous streamwise component of the Lamb vector at both wall-normal locations. The mean values of $T^+ \approx {[u \times \omega]_1}^+$ are -0.006 and -0.008 at ${x_2}^+ = 110 (x_2 = 0.1\delta)$ and 575 ($x_2 = 0.5\delta$), respectively. These values are consistent with the values reported in previous studies in the literature (Klewicki 1989; Priyadarshana *et al.* 2007).

A simple error propagation analysis (based on equation (1.4)) was performed to evaluate the uncertainty in T at a single point. The analysis indicates that this is dominated by the uncertainty in computing the fluctuating vorticity components. The relative uncertainty in the root-mean-square (r.m.s) value of T is approximately 20%. This is consistent with the results of Ganapathisubramani *et al.* (2005*b*) who found that the relative uncertainty in the fluctuating vorticity components is approximately 15–20%. This is also consistent with the results of Westerweel (1994) who found

that the vorticity values can be computed with an accuracy of 10–20% at best (depending on the measurement noise), provided the velocity data are within 1–2% accuracy. It must be noted that the relative uncertainty in regions that exhibit strong source- or sink-like character (i.e. regions where the instantaneous magnitude of T is significantly larger than the r.m.s value of T) is appreciably lower than the above uncertainty estimate.

The first measurement plane, $x_2^+ = 110$ ($x_2/\delta = 0.1$), is located in the log region and the second plane, $x_2^+ = 575$ ($x_2/\delta = 0.5$), is located in the wake region of the boundary layer. However, given that the results in the current study are presented in the context of momentum sources and sinks, distinction of wall-normal locations based on the traditional classification of log/wake layers may not be appropriate. Perhaps the wall-normal locations investigated in the current study should be classified based on the four-layer structure observed by Wei *et al.* (2005). If so, then the wall-normal locations are in Layer IV, which is the inertial/advection balance layer that ranges between $x_2^+ \approx 2.6\sqrt{\delta^+}$ and $x_2^+ = \delta^+$ (see Wei *et al.* 2005, p. 308, section 2.2 for details on the physical extent of the four layers).

3. Results

The spatial structure of T and its relationship with the velocity fluctuations can be explored by computing two-point auto- and cross-correlations. The two-point correlation (R) between two quantities is defined as

$$R_{AB}(\Delta x_1, \Delta x_3) = \frac{\overline{A(x_1, x_3)B(x_1 + \Delta x_1, x_3 + \Delta x_3)}}{\sigma_A \sigma_B} \tag{3.1}$$

where, σ_A and σ_B are the standard deviations of A and B, respectively, and Δx_1 and Δx_3 are the in-plane separations between the two quantities. The overline notation represents an ensemble average over multiple realizations. Note that a positive Δx_1 corresponds to correlation (R_{AB}) of variable B at a downstream location from variable A and a negative Δx_1 characterizes an upstream location of B with respect to A. A similar sign convention applies to the spanwise direction.

Note the correlations are computed by using the instantaneous values of T (and not the fluctuations of T about the local mean value). This is done to ensure that the source- and sink-like character of T is retained and the correlations can be interpreted directly.

Figures 1(a) and 1(b) show two-point auto-correlations R_{TT} at $x_2^+ = 110$ and 575, respectively. At $x_2^+ = 110$, the correlation contours are symmetric along both the streamwise and spanwise directions and appear spatially compact with a size of approximately 150 wall units. Additionally, the correlation reveals negative values in the spanwise direction at a distance of ± 100 wall units. This suggests that sink/source motions flank the source/sink-type motions. At $x_2^+ = 575$, the streamwise extent of the contours is comparable to that at $x_2^+ = 110$; however, the contours are wider in the spanwise direction, indicating that the spanwise length scale of the momentum sources/sinks increases with wall-normal distance.

The spatial structure of T can be further investigated by examining the contributions of source- and sink-like motions individually. This can be done by computing correlations conditioned on the sign of T, i.e. compute the two-point correlation R_{TT} such that $T(0, 0) > 0$ for source-like motions and $T(0, 0) < 0$ for sink-like motions. This not only reveals the structure of source- and sink-like motions but can also provide insight into the spatial organization of these motions with respect

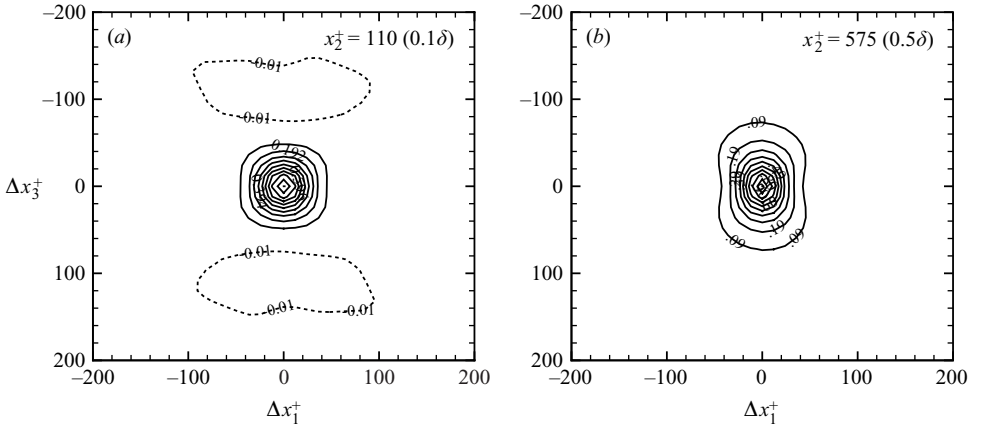

FIGURE 1. Two-point auto-correlation R_{TT} at (*a*) $x_2{}^+ = 110$ and (*b*) $x_2{}^+ = 575$. Negative levels are depicted with dashed lines.

to each other. Figures 2(*a*) and 2(*b*) show conditional two-point correlations at $x_2{}^+ = 110$, conditioned on the presence of source- and sink-like motions at the origin, respectively. The conditional correlation has a maximum value (at the origin) of 0.48 and 0.52 in figures 2(*a*) and 2(*b*), respectively, suggesting a very marginal dominance of sink-like motions at this wall-normal location. This is consistent with the fact that the mean value of T is negative at this location.

The positive contours in both figures are compact and similar to those observed in figure 1(*a*), indicating that strong source- and sink-like motions possess similar length scales. Figure 2(*a*) indicates negative values in the upstream direction as well both spanwise directions. In contrast, figure 2(*b*), which shows the conditional correlation for sink-like motions ($T < 0$), shows negative correlation values only in the downstream direction. This suggests that source-like motions are surrounded by sink-like motions in three directions.

In order to quantify the size of these source/sink motions, a representative length scale is chosen based on the correlation coefficient. This scale is defined as the full width of R_{AB} at a contour level equal to 0.1. The streamwise representative length scale is approximately 70 wall units for both $T > 0$ and $T < 0$. The spanwise length scales are 70 and 80 wall units for $T > 0$ and $T < 0$, respectively. The values are consistent with the previous observation that the sizes of source and sink motions are comparable.

Figures 2(*c*) and 2(*d*) show conditional two-point correlations of source- and sink-like motions at $x_2{}^+ = 575$. The maximum correlation values for $T > 0$ and $T < 0$ are 0.4 and 0.6, respectively, confirming that sink-like motions are dominant farther away from the wall. The positive contours extend farther in both streamwise and spanwise directions for $T < 0$ when compared to $T > 0$. The negative contours for $T > 0$ in figure 2(*c*) suggest that source-like motions are encompassed by sink-type motions. This is presumably due to the fact that the mean value of T is less than zero and therefore the correlation coefficient would be negative beyond a certain separation.

The streamwise representative length scales at $x_2{}^+ = 575$ are 70 and 85 wall units for $T > 0$ and $T < 0$, respectively. This suggests that the streamwise extent for $T > 0$ at this wall-normal location is comparable to those observed in $x_2{}^+ = 110$, suggesting that the length scales of source-like motions do not vary between the two wall-normal

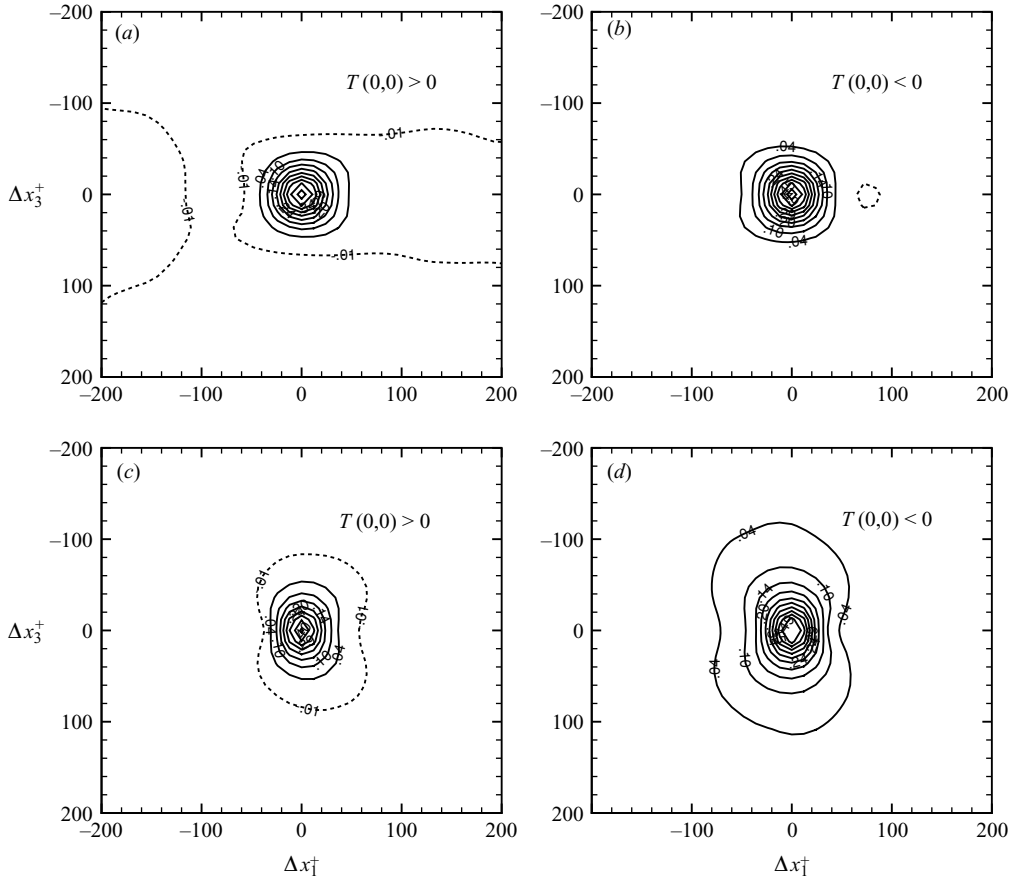

FIGURE 2. Conditional auto-correlation R_{TT} at $x_2{}^+ = 110$ for (a) $T(0,0) > 0$ and (b) $T(0,0) < 0$. Conditional auto-correlation R_{TT} at $x_2{}^+ = 575$ for (c) $T(0,0) > 0$ and (d) $T(0,0) < 0$. Negative contours are depicted with dashed lines.

locations examined in this study. In contrast, sink-like motions show a definite increase in length scale with wall-normal location. The spanwise representative length scales are 80 wall units for $T > 0$ and 135 wall units for $T < 0$, indicating that the sink motions are larger in the spanwise direction. Moreover, the spanwise length scale of both source and sink motions shows an increasing trend with wall-normal location.

The velocity field in a turbulent boundary layer is characterized by the presence of outward interactions (Q1 events, $u_1 > 0, u_2 > 0$), ejections (Q2 events, $u_1 < 0, u_2 > 0$), inward interactions (Q3 events, $u_1 < 0, u_2 < 0$) and sweeps (Q4 events, $u_1 > 0, u_2 < 0$). Various researchers have established the importance of each of these regions to turbulent kinetic energy. However, the impact of these regions on the mean–momentum balance has not been explored. Their role in the generation of source/sink motions can be explored by computing cross-correlations of T with the velocity components.

Figures 3(a) and 3(b) shows two-point correlations of T with u_1 and u_2, respectively, at $x_2{}^+ = 110$. Figure 3(a) shows that the correlation coefficient is positive in the vicinity of the origin and changes sign in both upstream and downstream directions. This suggests that source/sink-like motions appear in regions where u_1 changes sign in the

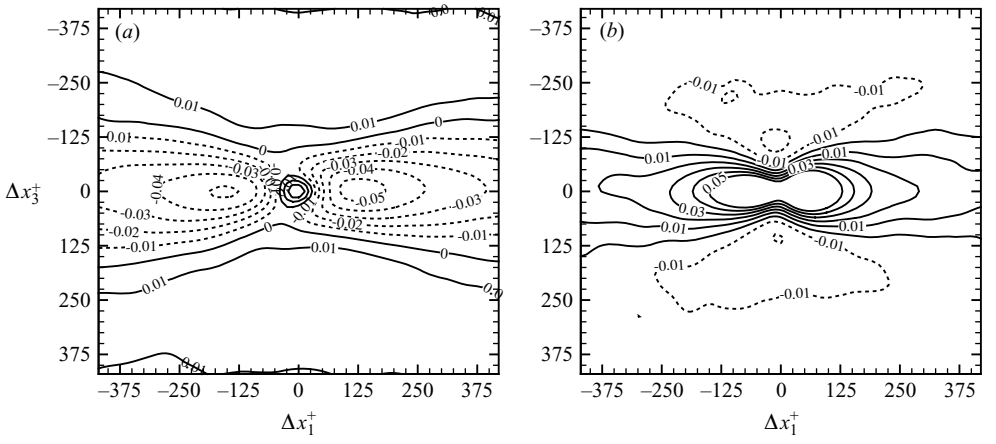

FIGURE 3. Cross-correlations at $x_2^+ = 110$, (*a*) R_{Tu_1} and (*b*) R_{Tu_2}. Contour levels from −0.05 to 0.05 are shown in increments of 0.01. Negative levels are depicted with dashed lines.

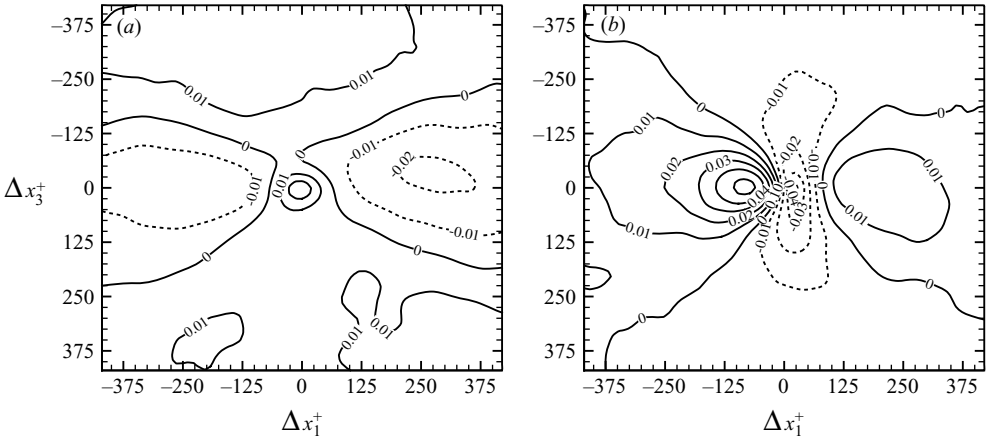

FIGURE 4. Cross-correlations at $x_2^+ = 575$, (*a*) R_{Tu_1} and (*b*) R_{Tu_2}. Contour levels from −0.05 to 0.05 are shown in increments of 0.01. Negative levels are depicted with dashed lines.

streamwise direction. This sign change occurs over a length of approximately 75 wall units. The correlation values change sign in the spanwise direction at a distance of approximately 100 wall units. This distance is comparable to the distance over which the two-point auto-correlation of u_1 changes sign (see Ganapathisubramani *et al.* 2005*a*). Figure 3(*b*) indicates that the u_2 velocity fluctuation does not undergo any sign change in the streamwise direction and reveals that the positive correlation contours extend in both upstream and downstream directions. However, the correlation values are found to change sign in the spanwise direction at a distance of 100 wall units similar to the change of sign observed in the R_{Tu_1} correlation in figure 3(*a*).

Figures 4(*a*) and 4(*b*) show two-point correlations of T with u_1 and u_2, respectively, at $x_2^+ = 575$. The R_{Tu_1} correlation contours at this wall-normal location are qualitatively similar to those found in figure 3(*a*) (at $x_2^+ = 110$). The correlation coefficient is positive in the vicinity of the origin and changes sign in both upstream and downstream directions. However, the correlation is not as strong as that at

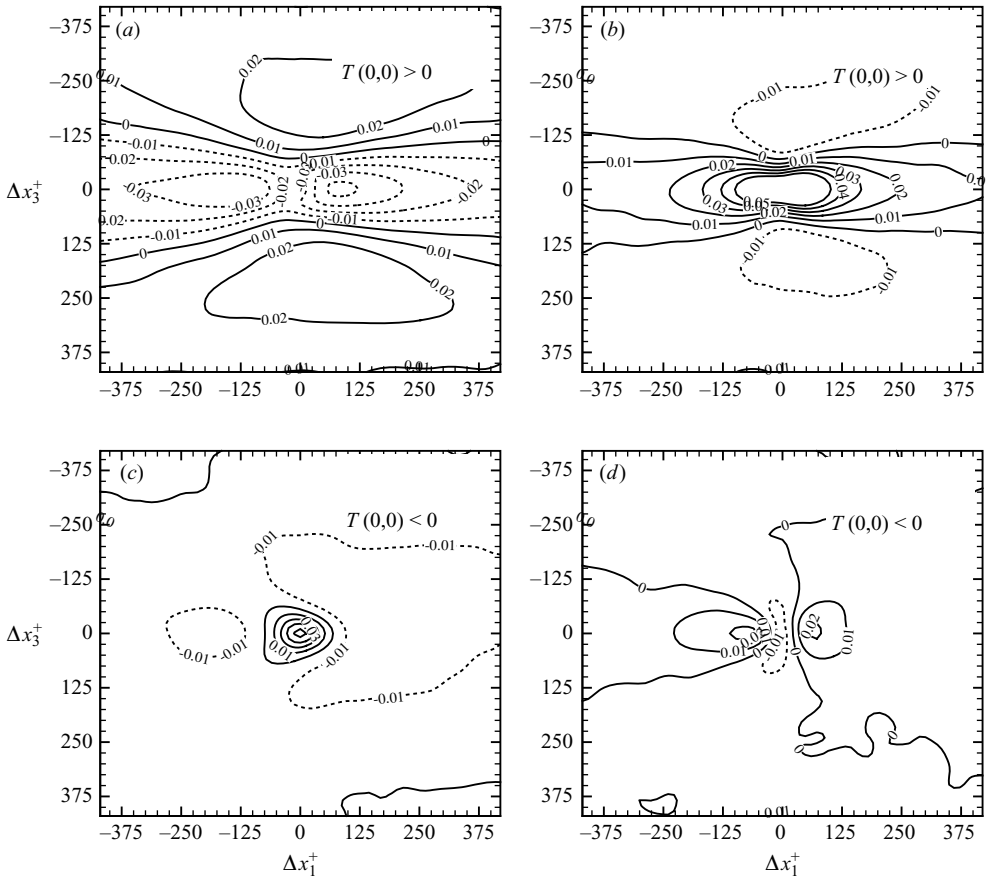

FIGURE 5. Conditional cross-correlations at $x_2{}^+ = 110$ for $T(0, 0) > 0$ (*a*) R_{Tu_1} and (*b*) R_{Tu_2}. For $T(0, 0) < 0$, (*c*) R_{Tu_1} and (*d*) R_{Tu_2}. Contour levels from -0.05 to 0.05 are shown in increments of 0.01. Negative contours are depicted with dashed lines.

$x_2{}^+ = 110$. The R_{Tu_2} correlation in figure 4(*b*) reveals negative values around the origin that extend in the spanwise direction up to $\Delta x_3 \approx \pm 250$ wall units. The streamwise extent of the negative correlation coefficient is about 100 wall units. This is markedly different from the structure of R_{Tu_2} at $x_2{}^+ = 110$ where the correlation coefficient was positive over an extended streamwise distance.

The structure of the velocity field can be further explored by computing conditional correlations. Figure 5(*a*) shows the correlation of $T > 0$ (i.e. source-like motions) with u_1 at $x_2{}^+ = 110$. This figure reveals that there is no positive correlation between $T > 0$ and u_1 in the vicinity of the origin, suggesting that the velocity fluctuations remain negative over an extended streamwise region. This reveals that the source-like motions are embedded within elongated low-momentum zones.

The correlation contours appear to have a neck at $\Delta x_1 = 0$, where they are found to converge for $\Delta x_1 < 0$ and diverge for $\Delta x_1 > 0$. Additionally, the correlation values depict a decreasing–increasing trend along $\Delta x_3 = 0$, indicating that the strength of u_1 fluctuations increases upstream and downstream of a source-like motion located at the origin. These two observations suggest that the elongated low-momentum zone meanders in the spanwise direction in the neighbourhood of the source-like motion. It is not clear if the presence of a source-like motion causes the meandering or

vice-versa. Regardless, this meandering nature of low-speed regions appears to be an integral part of source-like motions at this wall-normal location.

Figure 5(*b*) shows the conditional correlation of $T > 0$ with u_2 fluctuations at ${x_2}^+ = 110$. The figure reveals an elongated streamwise region of positive correlation suggesting that the source-like motions are located in the vicinity of upwash regions. The fact that the correlation values turn negative in the spanwise direction suggests the presence of downwash regions located on either spanwise side of a momentum source.

Figure 5(*c*) reveals the conditional correlation between $T < 0$ and u_1. The correlation coefficient is positive around the origin and negative values engulf this small area of positive correlation. The area of positive correlation extends about 80 wall units in both upstream and downstream directions. This indicates that the sink-like motions are associated with small regions of negative u_1 fluctuations that are embedded within a larger elongated region of positive u_1 fluctuations.

Figure 5(*d*), which shows the conditional correlation between $T < 0$ and u_2, indicates that sink-like motions are correlated with upwash events around the origin (negative correlation values) that are surrounded by larger regions of downwash (positive correlation contours). The negative correlation region is very thin in the streamwise direction (extending only 25–30 wall units). This observation, together with the size of the positive correlation region in figure 5(*c*), suggests that the velocity field undergoes a rapid transition in the neighbourhood of sink motions. The velocity field can be characterized by the presence of Q4 events farther away from the origin. The structure becomes Q3 events on either side of the origin and subsequently becomes Q2 events in the near vicinity of $\Delta x_1 = 0$. This velocity signature can be explained by the presence of a small region of upwash (that could be associated with a head of a hairpin-type vortex) located within an elongated high-speed region.

Figures 6(*a*) and 6(*b*) show conditional correlations of $T > 0$ with u_1 and u_2 and figures 6(*c*) and 6(*d*) show conditional correlations of $T < 0$ with u_1 and u_2 at ${x_2}^+ = 575$. Figures 6(*a*) and 6(*c*) indicate that source-like and sink-like motions are correlated with negative velocity fluctuations and that the two-point correlation in figure 4(*a*) that indicates a zero crossing in the correlation is misleading. In fact, the sign change occurs due to the dominance of sink-like motions (i.e. $T < 0$) at this wall-normal location.

The distinctive difference between source- and sink-like motions at this wall-normal location is in their correlation with u_2. The $T > 0$ events in figure 6(*b*) are correlated with extended regions of upwash (i.e. $u_2 > 0$) and is qualitatively similar to the structure observed at ${x_2}^+ = 110$. However, the size of structure at this wall-normal location is much larger and is consistent with fact that the size of two-point auto-correlations of u_2 increases with increasing wall-normal distance (see Ganapathisubramani *et al.* 2005*a*). The correlation between $T < 0$ events and u_2 reveals a sign change along the streamwise direction. The correlation coefficient is negative close to the origin and extends farther in the downstream direction. A profile of R_{Tu_2} along $\Delta x_3 = 0$ indicates that the correlation is positive for ${\Delta x_1}^+ < -100$ and is negative for $-100 < {\Delta x_1}^+ < 300$ and is positive beyond ${\Delta x_1}^+ > 300$. This signature is similar to the structure of R_{Tu_2} at ${x_2}^+ = 110$; however, the streamwise and spanwise length scales of the negative correlation are much larger.

4. Summary and discussion

The spatial structure of momentum source/sink-like motions is examined in the outer region of a turbulent boundary layer by computing two-point correlations.

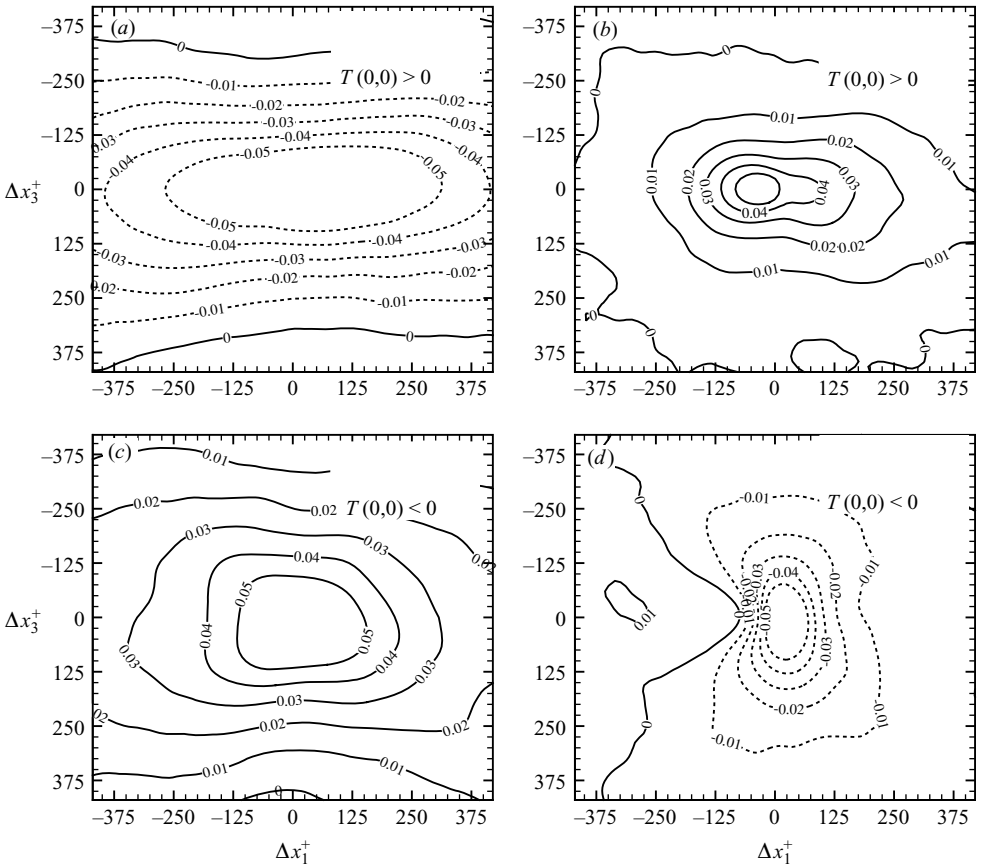

FIGURE 6. Conditional cross-correlations at $x_2^+ = 575$ for $T(0,0) > 0$ (*a*) R_{Tu_1} and (*b*) R_{Tu_2}. For $T(0,0) < 0$, (*c*) R_{Tu_1} and (*d*) R_{Tu_2}. Contour levels from -0.05 to 0.05 are shown in increments of 0.01. Negative contours are depicted with dashed lines.

Conditional correlations indicate that the streamwise length scale of source-like motions remains relatively constant whilst sink-like motions reveal an increasing trend with wall-normal distance. The spanwise length scales of both source and sink motions increases with wall-normal distance. Moreover, the strength of momentum sinks increases with distance from the wall, consistent with the observations based on the profile of mean Reynolds shear stress.

Momentum sources are correlated with elongated low-speed zones that possess regions of upwash embedded within them. Source-like motions appear to be the strongest in areas where the low-momentum zones meander in the spanwise direction. Their spanwise length scales are much larger at $x_2^+ = 575$ than at $x_2^+ = 110$. Momentum sinks also appear in low-momentum zones; however, the velocity signature is markedly different when compared to the signature in the vicinity of source-like motions. Sink-like motions appear in small regions of strong upwash that are embedded within larger high-momentum zones. These small regions of upwash can be associated with a spanwise head of a hairpin-type vortex located within an elongated high-speed region. Both streamwise and spanwise length scales are considerably larger at $x_2^+ = 575$ than at $x_2^+ = 110$.

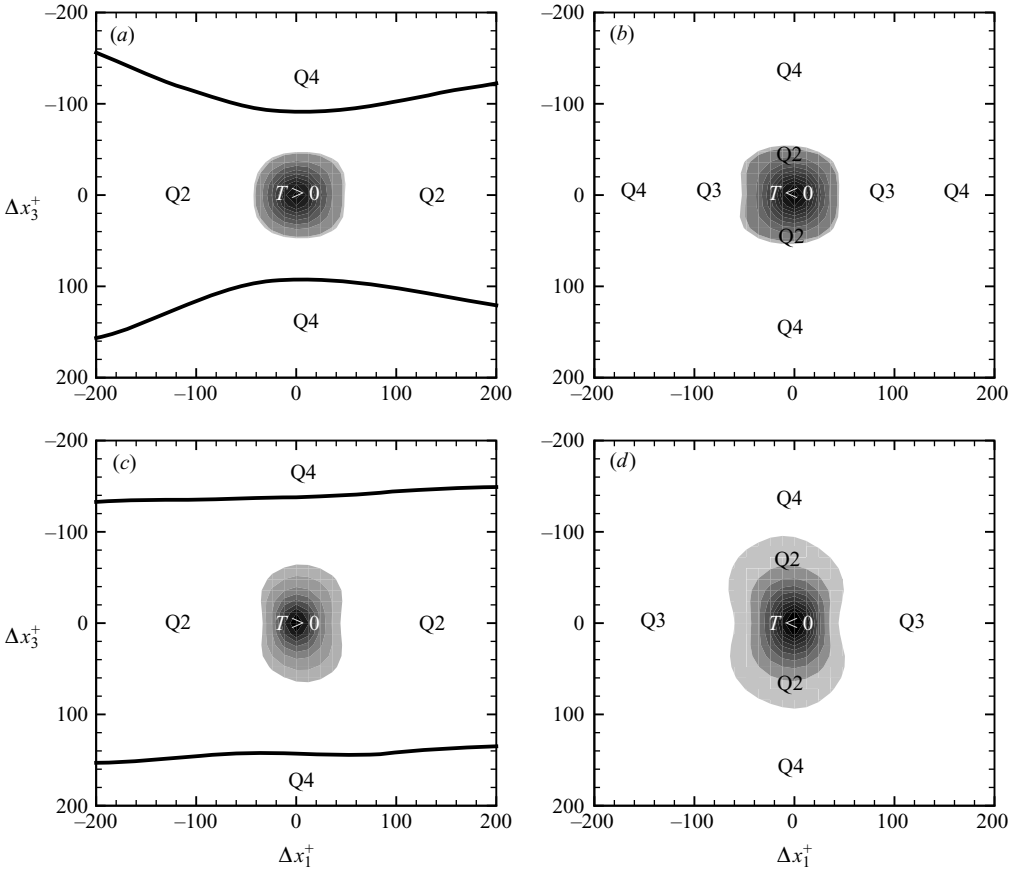

FIGURE 7. Schematic representations of $u_1 - u_2$ quadrant motions in the vicinity of source- and sink-like motions at the two wall-normal locations: $(a, b)x_2^+ = 110$, $(c, d)x_2^+ = 575$.

The observations based on the correlation structure suggest that the source and sink motions appear due to small-scale fluctuations in the velocity components in the presence of large-scale structures. This is consistent with the view presented by Hutchins & Marusic (2007) where they show that the large-scale motions have a distinct modulating influence on the small scales.

A plausible physical interpretation based on the correlation structure of momentum sources and sinks is as follows: Figure 7 shows schematic representations of $u_1 - u_2$ quadrant motions in the vicinity of source- and sink-like motions. The velocity signature of source-like motions in figures 7(a) and 7(c) are associated with elongated low-momentum zones with embedded regions of upwash. Strong source-like character is exhibited when these low-momentum zones meander in the spanwise direction (as shown by the converging–diverging contour lines in figure 7a). The spanwise scale of these elongated zones increases with wall-normal direction and the meandering nature of these structures appears to be inhibited. Consequently, the strength of source-like motions decreases farther away from the wall. This observation is also consistent with the fact that source-like motions dominate near the wall (the mean value of T is greater than zero near the wall) where the low-speed streaks reveal a meandering structure. Figures 7(b) and 7(d) show that the sink-like motions are

associated with areas that undergo various transitions. A primary characteristic of the velocity field appears to be the sign change exhibited by the wall-normal velocity fluctuation. At $x_2^+ = 110$, the velocity field exhibits a quadrant transition of the form, Q4–Q3–Q2–Q3–Q4, along the streamwise direction as seen in figure 7(*b*). At $x_2^+ = 575$, the velocity field reveals a Q3–Q2–Q3 signature (figure 7*d*). This observed difference could be attributed to the limited field of view at $x_2^+ = 575$. This velocity signature could be due to the presence of spanwise heads of hairpin-type vortices that are embedded within larger low-momentum zones. The induced velocities of these spanwise heads could trigger the quadrant transitions in figure 7.

The above physical description is consistent with the observations of Meinhart & Adrian (1995) who examined instantaneous velocity fields in the streamwise–wall-normal plane of a turbulent boundary layer and found the presence of uniform momentum zones separated from each other by thin viscous shear layers that contain concentrations of spanwise vorticity. Recently, Priyadarshana *et al.* (2007) noted that the appearance of source- and sink-like behaviour depends on the interactions between these uniform-momentum zones and the thin vorticity layers. The current study reveals the velocity signature in the vicinity of these interactions and indicates that source- and sink-like motions exhibit different features. Overall, the source and sink motions arise due to the presence of small-scale velocity fluctuations in the presence of a large-scale uniform-momentum zone. The interaction between small- and large-scale fluctuations induces rapid quadrant transitions and appears to result in source- and sink-like motions.

The author is grateful to Professor E. K. Longmire and Professor I. Marusic for all their support and Professor J. F. Morrison for many invaluable suggestions. He also acknowledges the referees for their comments and suggestions that aided in improving the quality of this paper.

REFERENCES

Adrian, R. J., Meinhart, C. D. & Tomkins, C. D. 2000 Vortex organization in the outer region of the turbulent boundary layer. *J. Fluid Mech.* **422**, 1–53.

Blackwelder, R. F. & Kaplan, R. E. 1976 On the wall structure of the turbulent boundary layer. *J. Fluid Mech.* **76**, 89–120.

Ganapathisubramani, B. 2004 Investigation of turbulent boundary layer structure using stereoscopic particle image velocimetry. PhD thesis, University of Minnesota, USA.

Ganapathisubramani, B., Hutchins, N., Hambleton, W. T., Longmire, E. K. & Marusic, I. 2005*a* Investigation of large-scale coherence in a turbulent boundary layer using two-point correlations. *J. Fluid Mech.* **524**, 57–80.

Ganapathisubramani, B., Longmire, E. K. & Marusic, I. 2006 Experimental investigation of vortex properties in a turbulent boundary layer. *Phys. Fluids* **18**, 055105.

Ganapathisubramani, B., Longmire, E. K., Marusic, I. & Pothos, S. 2005*b* Dual-plane PIV technique to measure complete velocity gradient tensor in a turbulent boundary layer. *Exps. Fluids* **39**, 222–231.

Guala, M., Hommema, S. E. & Adrian, R. J. 2006 Large-scale and very-large-scale motions in turbulent pipe flow. *J. Fluid Mech.* **554**, 521–542.

Hinze, J. O. 1975 *Turbulence*. McGraw-Hill.

Hutchins, N. & Marusic, I. 2007 Large-scale influences in near-wall turbulence. *Phil. Trans. R. Soc. Lond.* A **365**, 647–664.

Kim, K. C. & Adrian, R. J. 1999 Very large-scale motion in the outer layer. *Phys. Fluids* **11**, 417–422.

KLEWICKI, J. C. 1989 Velocity-vorticity correlations related to the gradients of the Reynolds stresses in parallel turbulent wall flows. *Phys. Fluids* A **1**, 1285–1288.

KLEWICKI, J. C. & HIRSCH, C. R. 2004 Flow field properties local to near-wall shear layers in a low Reynolds number turbulent boundary layer. *Phys. Fluids* **16**, 4163–4175.

KLEWICKI, J. C., MURRAY, J. A. & FALCO, R. E. 1994 Vortical motion contributions to stress transport in turbulent boundary layers. *Phys. Fluids* **6**, 277–286.

MEINHART, C. D. & ADRIAN, R. J. 1995 On the existence of uniform momentum zones in a turbulent boundary layer. *Phys. Fluids* **7**, 694–696.

NA, Y., HANRATTY, T. J. & LIU, Z. 2001 The use of DNS to define stress producing events for a turbulent channel flow over a smooth wall. *Flow Turbul. Combust*. **66**, 495–512.

ONG, L. 1992 Visualization of turbulent flows with simultaneous velocity and vorticity measurements. PhD thesis, University of Maryland, USA.

PRIYADARSHANA, P. J. A., KLEWICKI, J. C., TREAT, S. & FOSS, J. 2007 Statistical structure of turbulent boundary layer velocity-vorticity products at high and low Reynolds numbers. *J. Fluid Mech.* **570**, 307–346.

RAJAGOPALAN, S. & ANTONIA, R. A. 1993 Structure of the velocity field associated with the spanwise vorticity in the wall region of a turbulent boundary layer. *Phys. Fluids* **5**, 2502–2510.

ROVELSTADT, A. L. 1991 Lagrangian analysis of vorticity transport in a numerically simulated turbulent channel flow. PhD thesis, University of Maryland, USA.

THEODORSEN, T. 1952 Mechanism of turbulence. In *Proc. Second Midwestern Conference on Fluid Mechanics, March 17–19*. Ohio state Univesity, Columbus, Ohio.

WALLACE, J. M., ECKELMANN, H. & BRODKEY, R. S. 1972 The wall region in turbulent shear flow. *J. Fluid Mech.* **54**, 39–48.

WEI, T., FIFE, P., KLEWICKI, J. C. & MCMURTRY, P. 2005 Properties of mean momentum balance in turbulent boundary layer, channel and pipe flows. *J. Fluid Mech.* **522**, 303–327.

WESTERWEEL, J. 1994 *Digital Particle Image Velocimetry - Theory and Applications*. Delft University Press.

WILLMARTH, W. W. & LU, S. S. 1972 Structure of the reynolds stress near the wall. *J. Fluid Mech.* **55**, 65–92.